Available online at www.sciencedirect.com
SCIENCE DIRECT®
Journal of Chromatography A, 1080 (2005) 192–198
JOURNAL OF CHROMATOGRAPHY A
www.elsevier.com/locate/chroma

Integrated capillary electrophoresis amperometric detection microchip with replaceable microdisk working electrode
II. Influence of channel cross-sectional area on the separation and detection of dopamine and catechol

Yurong Wang, Hengwu Chen *

The Institute of Micro Analytical Systems, Department of Chemistry, Zhejiang University, Xixi Campus, Hangzhou 310028, China

Received 10 March 2005; received in revised form 21 April 2005; accepted 3 May 2005

Abstract

The interference of separation high voltage with the electrochemical detection is a major challenge to the microchip capillary electrophoresis–electrochemical detection systems with end-channel detection mode. Using dopamine and catechol as model analytes, the influences of channel cross-sectional area and channel-to-electrode distance on the high-voltage interference, accordingly on the separation and detection performances of the microchip capillary electrophoresis–electrochemical detection system were investigated. With the increase of the channel cross-sectional area from 312 through 450–615 μm^2, the apparent half-wave potentials of hydrodynamic voltammetry for dopamine at the field strength of 288 V/cm shifted positively from 285 through 330–400 mV. By using a chip with the smallest channel cross-section (312 μm^2 with top width of 37.3 μm and depth of 8.9 μm) the residual high-voltage field in the detection cell was small, so that detection was conducted at a channel-to-electrode distance of 20 μm to achieve better performances of separation and detection.

Keywords: Microchip capillary electrophoresis; Amperometric detection; High voltage interference; Dopamine and catechol

1. Introduction

Since the concept of miniaturized total analysis system (μ-TAS) was introduced [1,2], numerous papers have been published on microchip based analytical devices, of which the microchip capillary electrophoresis systems have achieved great growth. So far, laser induced fluorescence (LIF) [3] has been a predominating detection mode for these systems. However, the compounds that can be detected by LIF without derivatization are limited. Moreover, the bulky and complex optical equipments required by LIF impede the integration of LIF with the microchips. Electrochemical detection in amperometric mode (ED) is an attractive alternative for microchip analysis owing to its impressive advantages, such as high sensitivity, no requirement of derivatization for many compounds, ideal compatibility with integration and miniaturization, and less expensive in instrumentation. Therefore, ED combined to microchip capillary electrophoresis (microchip CE–ED) has, in recent years, received increased attention. Several reviews [3–6] have been published since the first report on a capillary electrophoresis chip with integrated amperometric detection [7]. Like the conventional CE–ED systems, however, the microchip CE–ED faces a major challenge, that is, the high-voltage field interference with the amperometric detection. To eliminate or reduce the interference, some workers used off-channel detection mode in-cooperation of a field decoupler [8–11] or in-channel detection mode in combination with an electrically isolated potentiostat [12]. Most workers, however, employed end-channel detection mode [7,13–26] because

* Corresponding author. Fax: +86 571 88273496.
E-mail addresses: hwchen@zju.edu.cn, hwchen@mail.hz.zj.cn (H. Chen).

0021-9673/$ – see front matter © 2005 Published by Elsevier B.V.
doi:10.1016/j.chroma.2005.05.032

it is much more simple in chip fabrication and/or instrumentation in comparison to the off-channel and in-channel detection modes. The end-channel mode was adapted from the end-column detection mode, originally proposed by Ewing and coworkers [27] for conventional CE–ED with capillaries of internal diameter less than 5 μm. In this case, the interference of high-voltage with the end-column detection was found negligible. Based on their investigation into relationship between capillary internal diameter, high-voltage interference and noise level, Cassidy and coworker [28] demonstrated that the end-column detection could also be operated with 25 μm I.D. capillaries. Since then, capillaries with 25 μm I.D. have been prevalently employed for CE–ED with end-column detection due to the advantages of less risk of blockage and more convenience in alignment of working electrode to capillary exit, although some groups have shown the possibility of using 50 or 75 μm I.D. capillaries for CE-EC [29,30]. For the microchip CE–ED with end-channel detection, a variety of chips with channel width ranging 50–80 μm and channel depth ranging 15–20 μm have been reported [14,16,17,21–24], despite that chips with width of less than 35 μm and depth of less than 10 μm have been used by a few workers [25,26]. However, to our best knowledge, no systematic investigation has been reported into the effect of channel cross-sectional areas on the high-voltage field interference and accordingly on the separation and detection performances of the microchip CE–ED systems.

For microchip CE–ED with end-channel detection, accurate alignment of working electrode to channel exit is troublesome. Two approaches were usually employed for the alignment. One permanently integrates a thin-film working electrode inside the on-chip detection cell at the place close to the channel exit [7,13,16,19,22,25]. With this approach, no off-chip device was required to fix and align the electrode, but the electrode was unable to be polished upon fouling. The other separated the detection cell from the chip, and a replaceable disk [15,17,20,23] or thick-film [14,21] working electrode was mounted on and aligned by an off-chip device such as an *XYZ* translation stage [15,23], an electrode-aligning slot [14,21] or a electrode-guiding tube [17]. Whenever the electrode was fouled, the working electrode could be removed to be polished or even replaced. However, the off-chip detection cell and the extra device for fixing and alignment of working electrode limited the degree of integration and miniaturization of the microchip CE–ED systems. In our previous work [31], we developed an integrated CE–ED chip with an on-chip electrode-orientating-bore that was used to mount and align a replaceable micro-desk working electrode. Without any off-chip device, the working electrode could be replaced in a couple of minutes and the reproducibility of the electrode alignment was better than 6% in RSD. A similar glass CE–ED chip, where a guiding-hole was etched with HF solution to hold the working electrode, was later reported by Wu et al. [32].

In the present work, the integrated CE–ED chip with the electrode-orientating-bore was made with different channel widths and depths, and the effect of high-voltage on the separation and detection performances was investigated with these chips of different channel cross-sectional areas by using dopamine and catechol as model analytes.

2. Experimental

2.1. Apparatus

A model of Dektek^3 profile-meter (Veeco Instruments Inc., woodbery, New York, USA) was used to measure the width and depth of the channels. A model GY-63 four-channel programmable high-voltage supplier (the supplied voltages ranging from −3000 to +3000 volts, Research Center for Analytical Sciences, Northeastern University, Shenyang, China) was employed to perform sample injection and separation. A CHI 812 electrochemical analyzer (CHI Instrument Co., Shanghai, China), equipped with a carbon fiber microdisk working electrode, a platinum wire (0.5 mm O.D.) counter electrode and a micro saturated Ag/AgCl reference electrode (Shanghai Kangning Electrode Co., Shanghai, China), was used for amperometric detection. A Lenovo P-II personal computer was employed to control the analyzer and collect data.

2.2. Chemicals

Dopamine (DA) and catechol (CA) were received from Sigma (St. Louis, MO, USA). Individual 10 mM stock solutions of DA and CA were prepared by dissolving the reagents in 0.1 M $HClO_4$. Working standards were daily prepared by dilution of the stock solutions to desired concentration with 30 mM K_2HPO_4/KH_2PO_4 solution (pH 7.0) that was also used as running buffer. All solutions for the electrophoresis experiments were filtered with 0.22 μm cellulose acetate film (Xinya Purifying Equipments Co., Shanghai, China) before use. All chemicals used were analytical grade or better. Deionized water was used to prepare all solutions.

2.3. Fabrication of microchip

The method used to fabricate the integrated glass microfluidic chips is detailed in Ref. [31]. Briefly, a design of cross channels was drawn with CorelDraw 9.0 software and printed onto a transparency using a laser-assisted image setter. The design on a transparency was transferred by UV exposure onto a 1.7 mm thick and 30 mm × 60 mm glass substrate (Shaoguang Microelectronics Corp., Changsha, China) that was purchased pre-coated with a thin chrome layer and positive AZ-1805 photoresist. The cross channel network was etched into the substrate in a well-stirred, dilute HF–NH_4F bath kept at 39 °C. At an etching rate of 1.4 μm/min, various channel widths and depths were made by controlling the etching time in 5–15 min. The formed cross channel network was composed of a long channel (56 mm) and a short chan-

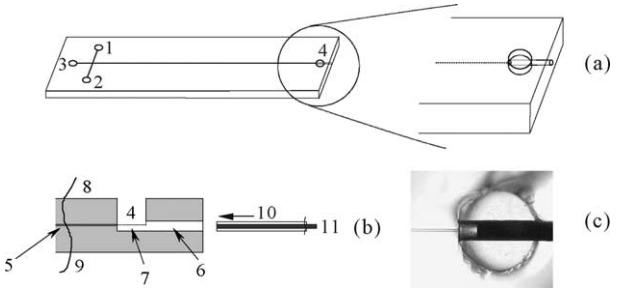

Fig. 1. Schematic diagram of the microchip with integrated electrochemical detection cell (a), the sectional view of the detection cell (b) and CCD image (bottom view) of the detection cell with a micro disk electrode positioning at a channel-to-electrode distance of about 400 μm (c). (1) Sample reservoir; (2) sample waste reservoir; (3) buffer reservoir; (4) detection reservoir; (5) separation channel; (6) orientating bore; (7) groove; (8) and (9) glass substrate; (10) fused-silica capillary and (11) carbon fiber micro-disk electrode.

nel (10 mm). The long channel was laid from the point 4 mm away the left edge of the chip down all the way to the right edge, and the short channel crossed the long channel at the middle of the short one and 5 mm from the starting point of the long channel (see Fig. 1a). Access holes of 1 mm I.D. for buffer, sample and sample waste reservoirs were drilled on the channel-structured substrate as usual. The fourth access hole for waste (also served as detection cell) was drilled on the substrate at the position 4 mm away from the right edge of the substrate, dividing the long channel into two sections: one was a 47 mm long (from the cross point to the waste cell) separation channel and the other was a 3 mm long orientating channel that would later be enlarged to an orientating bore. A flat glass substrate of the same type and size was used as the cover substrate. After being thoroughly cleaned, the structured substrate and the flat substrate were thermally bonded at 550 °C. Then, the right edge of the bonded chip was smoothed with an abrader. Using the method [33] for fabrication of a capillary-connecting bore in glass chip, an orientating bore was drilled with a 0.35 mm O.D. hard alloy steel drill along the orientating channel in the bonded chip. In the bottom of waste access hole, a semi-circular groove was drilled when the tip of drill bored into the area of waste hole. The groove terminated just outside the exit of the separation channel. The drilling process was monitored with a microscope. The completed chip was cleaned ultrasonically in water to remove all glass powder remaining in the bore and groove. Four pieces of plastic tube of 5 mm × 4 mm I.D. were respectively glued to the four access holes as buffer, sample, sample waste and waste reservoirs. The microchip design utilized in this work is illustrated in Fig. 1 (the plastic reservoirs are not shown).

2.4. Working electrode preparation

Multistrand carbon fiber microdisk electrodes were constructed with 6 μm O.D. carbon fibers. A bundle (about 30–40 fibers) of 30 mm long carbon fibers were carefully inserted into a 20 mm length × 250 μm I.D. and 375 μm O.D. fused-silica capillary (Refine Chromatography Ltd., Yongnian, Hebei, China), from one terminal (connection terminal) of the capillary until the fibers protruded from the other terminal (detection terminal) of the capillary. Epoxy glue was applied to both terminals of the capillary to fix the carbon fiber. The connection terminal was then inserted into a 15 mm length × 1 mm I.D. and 2 mm O.D. open glass tube until 1/4 length of the capillary was sheathed in the glass tube. Epoxy was used to seal the gap between the capillary and the glass tube. A piece of copper wire was introduced into the glass tube from its other end to connect the fibers, and mercury was filled into the tube to ensure electrical conductance between the fibers and copper wire. Then the open end of the glass tube was enclosed with epoxy glue. After curing overnight, the carbon fibers protruding out of the detection terminal of the capillary was cut to a disk with a scalpel, and polished with a 6 # abrasive paper until its tip was flat. Finally the microdisk electrode was cleaned ultrasonically in ethanol and water, respectively, each for 5 min.

2.5. Mounting and aligning of working electrode

The fabricated carbon fiber microdisk working electrode was inserted into the orientating bore on the chip, moving towards the separation channel along the groove under the bottom of the detection cell until a desired distance (20–50 μm) between the disk surface of the electrode and the channel exit. This process was monitored with a microscope (50× magnification) equipped with a calibrated reticule. Owing to that the sheath capillary of the electrode well mated the orientating bore, no sealing material was applied to prevent the leakage of solutions out of the detection cell. Prior to use, the mounted working electrode was scanned between 0 and 0.4 V (versus saturated Ag/AgCl reference electrode) in 1 mM potassium ferricyanide solution containing 1 M KCl until a steady and well-defined sigmoidal voltammogram was obtained.

2.6. Electrophoresis procedures

Before electrophoresis, the channels of microchip were sequentially rinsed, by applied vacuum in the buffer reservoir, with 0.1 M NaOH solution for 30 min, water for 10 min and finally running buffer for 30 min. The reservoir for sample solution was cleaned and filled with sample solution and all other reservoirs were filled with running buffer. After the chip equipped with a working electrode was placed in a Farady cage, counter and reference electrodes were inserted into the detection reservoir for detection, and platinum cathode and anode wires were placed in each reservoir and served as a contact for power supply. For injections, a high positive potential (600 V) was applied to the sample reservoir for 5 s with the detection reservoir grounded while all other reservoirs floating. Separations were performed by applying a desired potential (1500–2000 V) to the buffer reservoir with the detection reservoir grounded, while the sample and sample

waste reservoirs were held at 70% of the potential applied to the buffer reservoir to avoid the possible leakage of analytes from the sample channel to separation channel. As soon as the voltage was switched to perform electrophoresis separation, the electrochemical analyzer was actuated to record signals.

Hydrodynamic voltammograms (HDVs) at various conditions (specified in the corresponding figure captions) were recorded for 0.1 mM dopamine and catechol. Usually, two replicates were run for each applied potential, and the mean current was plotted against the potential.

3. Results and discussion

3.1. Characterization of the integrated CE–EC chip

The CE–ED chips used in the present work feature an orientating bore fabricated on the chips to fix the working electrode, so that no extra off-chip equipments are required to fix and align the electrode. Owing to that the axis of both the orientating bore and the orientating groove was exactly in line with the axis of the separation channel, and that the inner diameter of the bore and the groove exactly matched to the out diameter of the capillary used as electrode sheath, the electrode may be self-aligned to the channel exit in both *x*- and *y*-axes when it was inserted to the bore and approached to the channel exit along the groove. The only dimension required for the electrode to be adjusted is the distance between the exit of the separation channel and the surface of the disk electrode. This can be easily achieved with the help of a microscope. Compared with the CE–ED chip reported in Ref. [32], the orientating bore fabricated with a drill was more accurate in internal diameter than the guiding hole etched with HF solution, so that no epoxy glue was required to fix the electrode and seal the gap between the hole and electrode.

To investigate the influence of the channel cross-sectional area on the performance of the microchip CE–ED system, three chips with different channel cross-sectional areas were fabricated by controlling the etching time. They were respectively referred to as Chip L, Chip M and Chip S, corresponding to large, medium and small channel cross-sectional areas, respectively. Table 1 shows the parameters of the channel geometry and the corresponding etching times for the three chips. Since the cross-sectional area of a 25 μm I.D. fused-silica capillary was 490 μm^2, the estimated cross-sectional area for Chip M was approximately equal to that of 25 μm I.D. fused-silica capillary, while the area for Chip L was larger than, and that for Chip S was less than that of the 25 μm I.D. fused-silica capillary.

It is known that the separation efficiency of CE is dependent on the electric field strength and that the highest electric field strength is usually restricted by the Joule-heating effect. To investigate the Joule-heating effect of the chips with different channel cross-sectional areas, Ohm plots (current versus voltage) were constructed for the three chips that were filled with a 30 mM (pH 7.0) phosphate buffer, and linear regression equations for the linear parts of the plotted current–voltage curves were established. The slopes, intercepts and correlation coefficients of the equations were 2.16, 0.51 and 0.9996 for Chip S, 3.92, 0.38 and 0.9998 for Chip M, and 4.69, 0.36 and 0.9996 for Chip L, respectively. As expected, the conductivity of the buffer-filled channels (expressed by the slopes of the current–voltage lines) was increased with the increase of channel cross-sectional areas. As a result, the Joule-heating effect was more significant for the channel with large cross section: the linear range of the current–voltage plot for Chip L merely extended up to 2.0 kV (equivalent to a field strength of 385 V/cm), while the range for chip M and chip S were up to 2.4 kV (462 V/cm) and 2.8 kV (539 V/cm), respectively. Therefore, Chip S with a narrow and shallow separation channel was preferred for obtaining high separation efficiency by using higher field strength. However, in the following study on comparison of the high voltage effect on amperometric detection among the three chips, the highest voltage applied was restricted to 2 kV.

3.2. Influence of cross section on the working electrode potential

For end-column CE–ED system, the eletrophoretic current may produce an iR drop at the detection area. As a result, the actual interfacial potential at the working electrode may be different from the potential applied by the potentiostat, and shifts in half-wave potential of hydrodynamic voltammetry

Table 1
Geometric parameters of the channels etched for different times

Chip symbol	Etching time (min)	Channel geometry parameters			
		Width (μm)	Depth (μm)	Width-to-depth ratio	Cross-sectional area[a] (μm^2)
L	11.7	48.9	14.4	3.40	615
M	9.0	43.1	11.7	3.68	445
S	5.5	38.9	8.9	4.37	312

[a] The cross section can be approximated to be composed of two sectors with radius D and a rectangle with length D and width $W - 2D$ (W and D represent the channel width and depth, respectively). Thus, the cross-sectional area S was calculated with the equation of $S = \pi D^2/2 + D(W - 2D)$

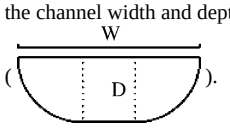

).

(HDV) may be observed when the HDV is performed in the presence of the high-voltage electric field. Lunte et al. [34] found a +130 mV shift in the half-wave potentials of HDVs for both dopamine and catechol when the voltage applied to a 50 cm × 25 μm I.D. capillary was increased from 15 to 30 kV. The authors pointed out that the shifts were affected by such experimental parameters as capillary-to-electrode distance and running buffer concentrations. Matysik [30] showed that the shift in working electrode potential for 50 μm I.D. capillaries was larger than that for 25 μm I.D. capillary. With respect to the microchip CE–ED systems, Wang et al. [14] reported a positive shift in the half-wave potentials of HDVs for dopamine upon the increase of high voltage.

To evaluate the influence of channel cross-sectional area on the apparent half-wave potentials, hydrodynamic voltammetry of dopamine was conducted with the three chips in the presence of 1500 V high voltage. Fig. 2 shows HDVs obtained in the tests. With the increase of the cross-sectional area, the half-wave potential for oxidization of dopamine was positively shifted from 0.285 V for Chip S through 0.330 for Chip M to 0.400 V for Chip L. It is clear that the larger the channel cross-sectional area the more positive the apparent half-wave potential. In the study on HDV performed in polymeric microchip, Wang et al. [35] observed that the oxidation current for dopamine rose at 0.3 V and reached the diffusion limited plateau at 0.9 V, the half-wave potential being 0.53 V. Thus, the slopes of the HDVs obtained in the present study for all the chips were sharper than, and the half-wave potentials were less positive than the corresponding values reported in Ref. [35]. One possible reason for this may be ascribed to the larger channel cross-sectional area (50 μm × 50 μm, square) of the polymer chip used in Ref. [35]. In the present study, the absolute shifts of the apparent half-wave potentials from that obtained in absence of high-voltage electric field could not be obtained because neither on-chip de-coupler was fabricated in the chips nor pressure driven was feasible for the channel network. Therefore, the difference between the apparent half-wave potentials with high voltage field applied and that without high voltage field could not be evaluated. To check whether or not the high-voltage field interference exists in Chip S, and if so how serious it is, the half-wave potentials for Chip S and Chip L observed at the high-voltage of 1500 V were respectively compared to those observed at the high-voltage of 2000 V. Tests indicated that a 500 V increase in the applied high voltage produced a + 45 mV shift in apparent half-wave potentials for the Chip S (see the insert part of Fig. 2) and that the same voltage increase led to + 75 mV shift in the half-wave potentials for Chip L (the corresponding HDVs are not shown). All the above data indicate that the smaller the channel cross section the lower the iR drop formed in the detection area. Despite that Chip S possesses the smallest channel cross-sectional area which is significantly less than not only that of a 25 μm I.D. fused-silica capillary but also that of most chips used in previous works on microchip CE–ED [13–17,19–23], the shift of half-wave potential caused by the applied high-voltage field can not be neglected. Thus, an optimized apparent potential applied to the working electrode for a specific microchip CE–ED system should be obtained by making a HDV plot under the selected conditions.

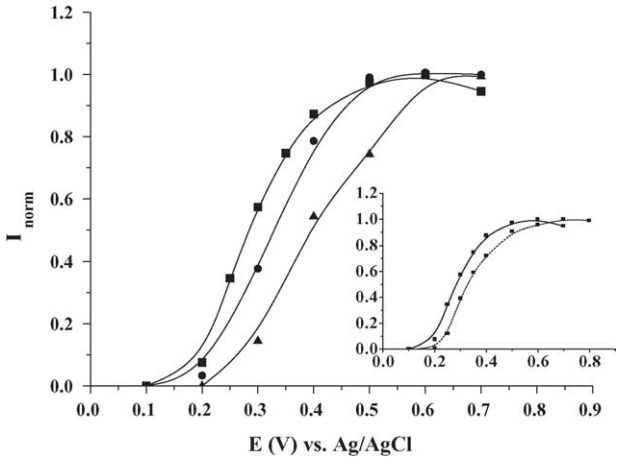

Fig. 2. HDVs for dopamine obtained with the three different chips at separation voltage of 1.5 kV (solid line) and 2.0 kV (dash line). Symbols: HDV obtained with Chip S (■), Chip M (●), and Chip L (▲). Conditions: dopamine concentration, 0.1 mM; buffer, 30 mM phosphate at pH 7.0; channel-to-electrode distance, 20 μm.

3.3. Influence of channel-to-electrode distance

The distance between capillary/channel exit and electrode tip is a critical parameter of CE–ED systems with end-column configuration. It influences not only the mass transport on the electrode surface but also the high-voltage electric field interference with the detection, consequently, the sensitivity, background level and separation efficiency. Detailed studies have been made by several groups [28,30,34] about the effect of capillary-to-electrode distance on the analytical performances for conventional CE–ED systems. As to the microchip CE–ED systems with end-channel detection configuration, the reported distance of channel-to-electrode adopted was usually in the range of 10–60 μm [13–17,19,20,24–26]. The large discrepancies in the reported distances may probably be due to differences in the channel and electrode configurations. Mathies's group [22], by using a sheath-flow to restrict the diffusion of the zones in the detection cell, extended the distance of the channel-to-electrode to 250 μm without loss in detection sensitivity.

In this work, the effect of channel-to-electrode distance on the high voltage field interference with the amperometric detection was investigated by performing HDVs of dopamine using two chips with different channel cross section areas and comparing the shifts in half-wave potentials. When the disk electrode moved close to the channel exit from a distance of 50–20 μm, a +15 mV shift in half-wave potential was observed for Chip S (see Fig. 3) in comparison to a +40 mV shift for Chip M (HDVs for Chip M are not given). Thus, the distance variation played rather slight influence on the ap-

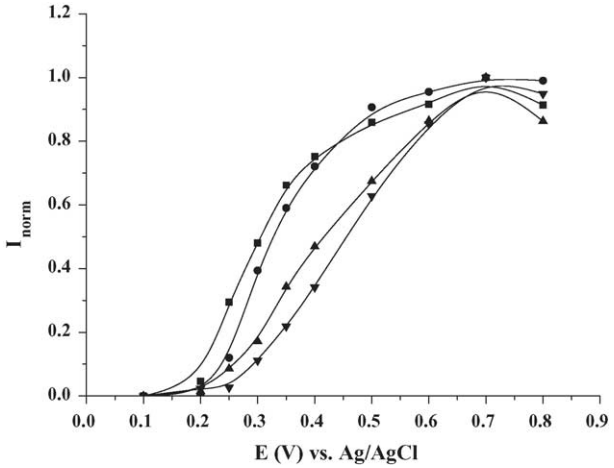

Fig. 3. HDVs for dopamine and catechol obtained with Chip S at different channel-to-electrode distances. Symbols: dopamine at channel-to-electrode distance of 50 μm (■) and 20 μm (●); catechol at 50 μm (▲) and 20 μm (▼). Conditions: analyte concentration, 0.1 mM; buffer, 30 mM phosphate at pH 7.0 and separation voltage, 2.0 kV.

parent potential of working electrode for the chip with small cross-sectional area. Masykis et al. [30] reported a similar observation for the conventional CE–ED. Further study on the effect of channel-to-electrode distance on the separation and detection performances was conducted with Chip S only. From the HDVs of dopamine and catechol obtained with Chip S (Fig. 3), a detection potential of +0.7 V versus a saturated Ag/AgCl reference electrode was selected, because the oxidization currents for both dopamine and catechol reached the diffusion-limited plateaus at the selected detection potential under the high voltage of 2000 V. Fig. 4 shows the electropherograms for the separation of dopamine and catechol obtained at the distance of 20 and 50 μm, respectively.

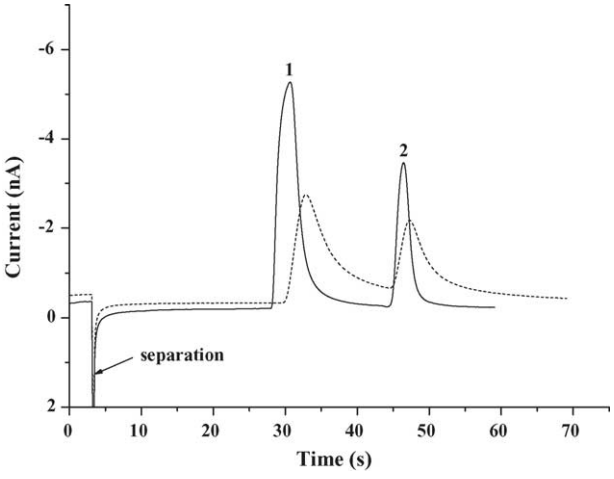

Fig. 4. Electropherograms of dopamine and catechol obtained at the channel-to-electrode distance of 20 μm (solid line) and 50 μm (dashed line). Peak identification, (1) for dopamine and (2) for catechol. Conditions: analyte concentration, 0.1 mM; buffer, 30 mM phosphate at pH 7.0; separation voltage, 2 kV; sample injection, 5 s at 600 V; working electrode potential, 0.7 V vs. saturated Ag/AgCl reference electrode.

Table 2
Analytical performances for dopamine (DA) and catechol (CA) observed at different channel-to-electrode distances

	DA		CA	
	20 μm	50 μm	20 μm	50 μm
t_m(s)	27.2	29.4	43.0	43.8
i_p (nA)	5.05	2.26	3.22	1.43
$W_{1/2}$ (s)	3.1	4.3	1.9	3.3
N (plate/m)	9.1×10^3	5.2×10^3	6.7×10^4	1.9×10^4
$\varphi_{1/2}$ (V)	0.330	0.308	0.458	0.420
Noise (pA)	6	5	6	5
LOD (μM, 3σ)	0.46	ND	0.94	ND

ND: not determined.

Corresponding data for the performances of separation and detection are listed in Table 2. As clearly shown in Fig. 4, with the increase of the channel-to-electrode distance from 20 to 50 μm, significant increase in both migration times and peak widths, and dramatic decrease in peak heights were observed. Thus, higher sensitivity and better separation efficiency could be achieved at the distance of 20 μm (Table 2). It was also noticed that the increase in migration times for DA was more significant than that for CA. This could be ascribed to the changes in velocities of DA and CA after they left the channel. Inside the separation channel, the positively charged species DA was driven by both electroosmosis and electrophoresis, while neutral species CA was driven by electroosmosis only. So in the channel DA migrated faster than CA. As soon as two species sequentially left the channel and entered the detection cell where almost no high voltage field existed, they were only pushed forwards by the in-channel generated electroosmotic flow. Thus DA significantly reduced its velocity due to disappearance of electrophoresis action. As a result, the increase in migration times caused by the increase in channel-to-electrode distance appeared more significant for DA than for CA. As for the noise level, no significant difference was observed at the two distances as listed in Table 2, despite that the noise level was significantly higher than Ref. [17] reported (0.5–1 pA was observed by using a 7 μm diameter carbon disk electrode).

The higher noise level can be attributed to the large detection area of the carbon fiber microdisk electrode. The similarity in the noise level may be explained that only a very small percentage of the high voltage dropped across the detection area of Chip S. Tests also showed that seven consecutive runs of a standard solution containing 0.1 mM dopamine and 0.1 mM catechol resulted in RSDs (relative standard deviations) of 0.75% (migration times) and 1.30% (current peak heights) for DA, and 1.08% (migration times) and 3.04% (current peak heights) for CA, respectively, under the conditions of 20 μm channel-to-electrode distance for the Chip S operated at the high voltage of 2000 V.

4. Conclusion

For microchip CE–ED systems with end-channel detection, the channel cross-sectional area strongly affects the

high voltage interference with the amperometric detection. The iR drop generated at the detection cell by the separation current and accordingly the shift in apparent half-wave potential of the working electrode was quite large for the chip with a channel top-width of 49 μm and depth of 14 μm, whose cross-sectional area was no more than that of the chips most widely-used for CE–ED systems. By reduction of the channel width and depth respectively to 39 and 9 μm, the high-voltage effect on the end-channel detection was significantly reduced and the performances of separation and detection improved. Since the iR drop was influenced not only by the cross-sectional area, but also by such experimental parameters as applied high voltage and channel-to-electrode distance, the optimal apparent potential applied to the working electrode for a specific microchip CE–ED system should be obtained by constructing a HDV plot under the selected conditions.

Acknowledgements

Natural Science Foundation of China (project No. 20299030 and No.20475048) and Natural Science Foundation of Zhejiang Province (project No. M203098) are thanked for funding this work. Prof. Zhaolun Fang and Miss Li Fan are thanked for improving the English writing for our manuscript.

References

[1] A. Manz, N. Graber, H.M. Widmer, Sens. Actuators B 1 (1990) 244.
[2] D.J. Harrison, K. Fluri, K. Seiler, Z. Fan, C.S. Effenhauser, A. Manz, Science 261 (1993) 895.
[3] M.A. Schwarz, P.C. Hauser, Lab. Chip 1 (2001) 1.
[4] W.R. Vandaveer, S.A. Pasas-Farmer, D.J. Fischer, C.N. Frankenfeld, S.M. Lunte, Electrophoresis 25 (2004) 3528.
[5] J. Wang, Talanta 56 (2002) 223.
[6] R.P. Baldwin, Electrophoresis 21 (2000) 4017.
[7] A.T. Woolley, K.Q. Lao, A.N. Glazer, R.A. Mathies, Anal. Chem. 70 (1998) 684.
[8] J.S. Rossier, R. Ferrigno, H.H. Girault, J. Electroanal. Chem. 492 (2000) 15.
[9] D.M. Osbourn, C.E. Lunte, Anal. Chem. 75 (2003) 2710.
[10] D.C. Chen, F.L. Hsu, D.Z. Zhan, C.H. Che, Anal. Chem. 73 (2001) 758.
[11] C.C. Wu, R.G. Wu, J.G. Huang, Y.C. Lin, H.C. Chang, Anal. Chem. 75 (2003) 947.
[12] R.S. Martin, K.L. Ratzlaff, B.H. Huynh, S.M. Lunte, Anal. Chem. 74 (2002) 1136.
[13] R.S. Martin, A.J. Gawron, S.M. Lunte, Anal. Chem. 72 (2000) 3196.
[14] J. Wang, B.M. Tian, E. Sahlin, Anal. Chem. 71 (1999) 5436.
[15] M.A. Schwarz, B. Galliker, K. Fluri, T. Kappes, P.C. Huauser, Analyst 126 (2001) 147.
[16] R.P. Baldwin, T.J. Roussel Jr., M.M. Crain, V. Bathlagunda, D.J. Jackson, J. Gullapalli, J.A. Conklin, R. Pai, J.F. Naber, K.M. Walsh, R.S. Keynton, Anal. Chem. 74 (2002) 3690.
[17] Y. Zeng, H. Chen, D.W. Pang, Z.L. Wang, J.K. Cheng, Anal. Chem. 74 (2002) 2441.
[18] Y. Liu, J.A. Vickers, C.S. Henry, Anal. Chem. 76 (2004) 1513.
[19] J.L. Yan, Y. Du, J.F. Liu, W.D. Cao, X.H. Sun, W.H. Zhou, X.R. Yang, E.K. Wang, Anal.Chem 75 (2003) 5406.
[20] N. Bao, J.J. Xu, Y.H. Dou, Y. Cai, H.Y. Chen, X.H. Xia, J. Chromatogr. A 1041 (2004) 245.
[21] A. Much Jr., J. Wang, M. Jacobs, G. Chen, M.P. Chatrathi, V. Jurka, Z. Výbomý, S.D. Spillman, G. Sridharan, M. Schöning, Anal. Chem. 76 (2004) 2290.
[22] P. Ertl, C.A. Emrich, P. Singhal, R.A. Mathies, Anal. Chem. 76 (2004) 3749.
[23] J.C. Fanguy, C.S. Henry, Electrophoresis 23 (2002) 767.
[24] R.S. Keynton, T.J. Roussel Jr., M.M. Crain, D.J. Jackson, D.B. Franco, J.F. Naber, K.M. Walsh, P.R. Baldwin, Anal. Chim. Acta 507 (2004) 95.
[25] D.P. Manica, Y. Mitsumori, A.G. Ewing, Anal. Chem. 75 (2003) 4572.
[26] N.E. Hebert, W.G. Kuhr, S.A. Brazill, Anal. Chem. 75 (2003) 3301.
[27] X.H. Huang, R.N. Zare, S. Sloss, A.E. Ewing, Anal. Chem. 63 (1991) 189.
[28] W.Z. Lu, R.M. Cassidy, Anal. Chem. 66 (1994) 200.
[29] A.M. Fermier, M.L. Gostowski, L.A. Colon, Anal. Chem. 68 (1996) 1661.
[30] F.M. Matysik, Anal. Chem. 72 (2000) 2581.
[31] F. Meng, H.W. Chen, Y.H. Dou, Z.L. Fang, Chem. J. Chinese Univ. 25 (2004) 844 (CA, 2004, 141:184244).
[32] Y.Y. Wu, J.M. Lin, R.G. Su, F. Qu, Z.W. Cai, Talanta 64 (2004) 338 (CA, 2004, 141:306602).
[33] N.H. Bings, C. Wang, C.D. Skinner, C.L. Colyer, P. Thibault, D.J. Harrison, Anal. Chem. 71 (1999) 3292.
[34] S.R. Wallenborg, L. Nyholm, C.E. Lunte, Anal. Chem. 71 (1999) 544.
[35] J. Wang, M. Pumera, M.P. Chatrathi, A. Escarpa, R. Konrad, A. Griebel, W. Dörner, H. Löwe, Electrophoresis 23 (2002) 596.